LUND UNIVERSITY

A Case Study on the Influence of Multiple Users on the Effective Channel in a Massive MIMO System

Bengtsson, Erik L; Flordelis i Minguez, José; Rusek, Fredrik; karlsson, Peter C.; Tufvesson, Fredrik; Edfors, Ove

A Case Study on the Influence of Multiple Users on the Effective Channel in a Massive MIMO System

Erik L. Bengtsson[1,2], Jose Flordelis[2], Fredrik Rusek[1,2], Peter C Karlsson[1], Fredrik Tufvesson[2], Ove Edfors[2]
[1]Radio Access Lab, Sony Mobile Communications, Lund, Sweden
[2]Dept of Electrical and Information Technology, Lund University, Lund, Sweden

Abstract—We investigate the importance of weak clusters when modeling a wireless massive MIMO channel. We do this by studying the influence of densely spaced terminals and the number of base-station antennas for a zero-forcing precoded massive MIMO system. In particular, we focus on the influence on the correlation and imbalance between the signals at the terminal antennas, the effective channel-gain, the eigenvalue distributions and the number of clusters. The study is based on measured radio-channels from terminal prototypes with integrated antennas connected to a massive MIMO testbed. We further evaluate the advantage of using block-diagonalized zero-forcing compared to conventional zero-forcing in a massive MIMO system. Unexpectedly, terminals with low antenna envelope correlation coefficient may benefit significantly from block-diagonal zero-forcing in a massive MIMO system. The main conclusion is that weaker clusters are important when modeling multi-user scenarios.

Index Terms—Terminal antenna, massive MIMO, zero-forcing, block-diagonalization, channel statistics, antenna pattern.

I. INTRODUCTION

Massive MIMO (MaMi) [1] is an essential part of the emerging new radio (NR) standard for the fifth-generation (5G) wireless communication [2]. MaMi has received a lot of attention in the wireless communication community [3]–[8] and suggests that capacity can be increased by an order of magnitude and energy-efficiency by two orders of magnitude. Except for a few papers [9]–[13], the terminal side of the MaMi system has not received much attention in the literature and relates mostly to idealized isotropically radiating single antenna terminals.

In [13] we proposed a cluster[1] based, link-level, MaMi simulation model that uses measured terminal-antenna characteristics. However, the scope of [13] was limited to a single terminal, although with multiple antennas, at a static physical location in space. It is, therefore, our ambition to extend the simulator, and this paper presents investigations of underlying channel properties that need to be accounted for. More specifically, in [20] the number of clusters is estimated using a channel sounder, but simplifications are made in [13] to include only clusters of significant power. This builds on the understanding that in the single-user (SU) case a zero-forcing

erik.bengtsson@sony.com, jose.flordelis@eit.lth.se, fredrik.rusek@eit.lth.se
peterc.karlsson@sony.com, fredrik.tufvesson@eit.lth.se, ove.edfors@eit.lth.se

[1]Based on observations of wireless channels, [14]–[16] contributions of signals propagating along various paths, a.k.a. multipath components (MPCs), tend to be clustered. This can be explained by the reflections caused by various objects in the environment. Numerous cluster-based simulation models for MIMO systems exist, e.g. [17]–[19].
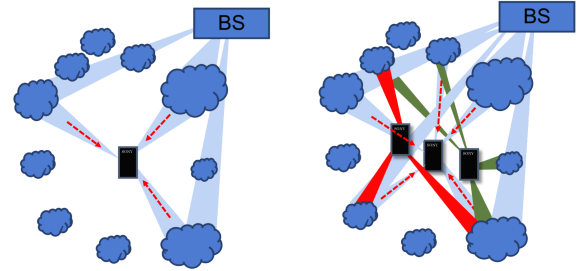

Fig. 1: Geometry-based cluster-model, where a few dominant clusters determine the effective channel at the terminal side (left), and a MU scenario where more clusters are used to separate the terminals (right).

(ZF) precoder allocates power according to the maximum ratio principle. This means that mainly dominant clusters are illuminated while weaker clusters become insignificant. If the number of terminals in a limited area increases, and thus a more complex precoding matrix needs to be utilized, the importance of the weaker clusters seen by each terminal grows. To separate terminals, also weaker clusters become significant in the effective channel and therefore need to be present in a model. From a MIMO perspective this is a plausible mechanism behind a better conditioned channel matrix, but with weaker eigenvalues. Furthermore, it is often unclear how many clusters are exclusive to a single terminal, and how many are common. Ultimately, our goal is to establish a multi-terminal simulator that assigns non-shared clusters to each terminal, seen only by that terminal, and shared clusters to a group of terminals, seen by all terminals in the group. Furthermore, we aim to include dependencies on: the distance between terminals, the distance to the basestation (BS), and the environment type. This is an important aspect in the multilink case of the COST 2100 channel model [18], and we apply it in a MaMi context. In general N shared clusters give N degrees of freedom. However, the condition of a simulated channel matrix may be hard to match to a measurement for some scenarios. With some of the clusters defined as individual clusters we can control the condition of the channel matrix, depending on how strong we make them, and a combination is therefore likely more realistic.

We identify properties that must be accounted for in simulations when multi-users (MU) are present, and analyze those in detail. Firstly, we investigate how other users influence the effective channel of an individual terminal. Secondly, we

perform an investigation of the relation between inter-terminal distance and the number of shared clusters.

Concerning the impact of other users on a single terminal, we aim to verify the following hypothesis: *When multiple terminals are introduced in a limited space, a ZF precoder causes a larger set of clusters to be illuminated.* The motivation behind this are the following facts and assumptions: For a SU MaMi case, the strongest effective channels for a dual-antenna terminal are given by the dominant eigenmodes of the channel. In a cluster/geometry-based channel model, this can be modeled as transmissions via a few dominant clusters (left of Fig. 1). In a MU MaMi system using zero-forcing (ZF) precoder, the eigenmodes of the effective channel between the terminal and the BS change. The channel typically becomes weaker when the precoder-rank is increased by the introduction of more terminals. The change of the eigenmodes is consistent with that when also weaker clusters are illuminated in the cluster-based model (right of Fig. 1).

We aim to verify the hypothesis by studying the effective correlation between the signals at the antennas of a terminal, which can then be expected to decrease and approach the envelope correlation coefficient [20] of the antennas.

The main contributions of this paper are:

- Our analyasis show that the measured radio channels do not have any signs of being limited to a few clusters, and the channel matrix, $\boldsymbol{H}$, seen from the BS side can be expected to have a high rank and should not be limited to a few clusters in the modeling process.
- We demonstrate that, in our measured scenario, two terminals at a distance of only 5 m share essentially no clusters, which means that the channel matrix, $\boldsymbol{H}$, seen from the BS side is well conditioned.
- We study empirically the advantage block-diagonal ZF (BDZF) [21] has over classical ZF (CZF) in MaMi systems and relate it to the terminal antenna correlation.

II. SET-UP AND EVALUATION MODEL

Since we deal with multiple terminals, we need some form of BS precoding. BDZF separates terminals without separating antennas within a terminal. BDZF, therefore, allows for evaluation of the influence terminals sharing the same channel have on the correlation and power imbalance between the antennas of a terminal. Loosely speaking, the performance of CZF is often assumed to approach the channel capacity as the number of BS antennas grows large [6] and, BDZF may therefore not be significantly better in MaMi systems.

A. Measurement Set-up

All measurements were conducted in an auditorium as shown in Fig. 2. Four measurement conditions were defined based on two terminals, each measured both stand-alone and loaded by a phantom head with a left hand (HHL). The terminal prototypes are based on Sony Xperia handsets with integrated antennas, tuned to the 3.7 GHz band used by the Lund massive MIMO testbed [22]. It can be noted that the envelope correlation coefficients between the antennas in both prototypes are close to zero. The terminals were transmitting
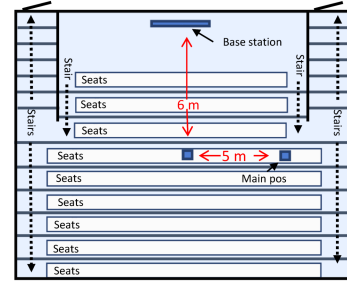

Fig. 2: Drawing of the auditorium where the measurements were performed.

pilot signals from both antennas to the testbed, and estimated transfer functions between all antennas, representing snapshots of the channel, were stored. Each snapshot corresponds to a unique terminal orientation, rotation angle, and location in the room. For the stand-alone captures, two different orientations were used, each measured at about 30 different rotation angles, giving $C_s \approx 60$ channel snapshots. For the HHL captures three different orientations were used, resulting in $C_s \approx 90$ channel snapshots. In all, about 300 different channel snapshots, each with two terminal-antennas, were logged for the four terminal-conditions. A snapshot contains 20 frequency samples, equally spaced over 20 MHz (i.e., the sub-carrier spacing is 1 MHz) for all terminal and BS antennas.

B. Experimental Evaluation

In the evaluations, one of the four measured terminal-conditions is considered being the reference. As the SNR of the measured channels was about 20 dB or more in all cases we ignore measurement noise and assume the measured channels to be the true ones. In each evaluation, the number of terminals, K, is increased from 1 to 10. With each terminal sharing the channel having two antennas, the total number of streams, therefore, increases from 2 to 20. For each realization, a randomly selected snapshot from the reference condition is combined with those of the $K - 1$ terminals. For each of the terminals, a random snapshot is selected, and all of the added terminals are different from the reference terminal. For each set of K terminals, 1000 realizations are generated and we record the medians of the correlation, power imbalance, and channel-gain (i.e., the trace of the inner product of the channel) between the antennas of the reference terminal.

The channels from terminal k are represented by an $M \times 2$ matrix, $\boldsymbol{H}_k$, where M is the number of BS antennas. For SU-MaMi, the channel properties are given by the inner product, $\boldsymbol{G}_k = \boldsymbol{H}_k^H \boldsymbol{H}_k$, which is a 2×2 matrix. Using the normalized version of the inner product, the terminal antenna correlation, α, and power imbalance, β can be identified [23]

$$\boldsymbol{G}_{\text{norm}} = \frac{2}{\text{tr}(\boldsymbol{G}_k)} \boldsymbol{G}_k = \begin{bmatrix} 1+\beta & \alpha \\ \alpha^* & 1-\beta \end{bmatrix}, \qquad (1)$$

where $\text{tr}(\cdot)$ is the trace operator.

For the MU-MaMi case, we adjoin the channel matrices from all terminals, each with two antennas, into a full channel matrix $\boldsymbol{H} = [\boldsymbol{H}_1 \boldsymbol{H}_2 \cdots \boldsymbol{H}_K]$. To find the space where the BS can perform transmissions to terminal k without causing interference to the other $K - 1$ terminals, we define

$\boldsymbol{H}_{\mathrm{I}|k} = [\boldsymbol{H}_1 \cdots \boldsymbol{H}_{k-1} \ \boldsymbol{H}_{k+1} \cdots \boldsymbol{H}_K]$, and compute its null-space, $\mathcal{N}_{\mathrm{space}|k}$. Assuming that $\boldsymbol{H}_{\mathrm{I}|k}$ has full rank, $\mathcal{N}_{\mathrm{space}|k}$ can be represented by an $M \times (M - 2(K-1))$ matrix $\boldsymbol{N}_{\mathrm{space}|k}$ with orthogonal columns. By multiplying the channel of terminal k, $\boldsymbol{H}_k$, with the null-space of the other terminals, $\boldsymbol{N}_{\mathrm{space}|k}$, we obtain the effective channel matrix for terminal k, $\boldsymbol{H}_{\mathrm{BD}k} = \boldsymbol{H}_k^{\mathrm{H}} \boldsymbol{N}_{\mathrm{space}|k}$, which is a $2 \times (M - 2(K-1))$ matrix. We can now compute the BD-based inner product $\boldsymbol{G}_{\mathrm{BD}} = \boldsymbol{H}_{\mathrm{BD}k} \boldsymbol{H}_{\mathrm{BD}k}^{\mathrm{H}}$, which is a 2×2 matrix that represents the interference free subspace for terminal k, for the BD precoder case. Normalizing $\boldsymbol{G}_{\mathrm{BDk}}$, the same way as in (1), the effective correlation, α_{BDk}, and power imbalance, β_{BDk} can be identified analogously to the SU-MaMi case. The term $\mathrm{tr}(\boldsymbol{G}_{\mathrm{BDk}})$ reflects the effective channel-gain seen by the terminal antennas, which we refer to as γ.

Similarly, to compute the effective channel in the CZF case, for a given terminal antenna l, $1 \leq l \leq 2K$, we define the matrix, $\boldsymbol{H}_{\mathrm{I}|l} = [\boldsymbol{H}_1 \cdots \boldsymbol{H}_{l-1} \ \boldsymbol{H}_{l+1} \cdots \boldsymbol{H}_{2K}]$. We follow the same steps as above but use the null-space of $\boldsymbol{H}_{\mathrm{I}|l}$ as our precoder. For terminal antenna l, $\boldsymbol{H}_{\mathrm{ZF}l} = \boldsymbol{H}_l^{\mathrm{H}} \boldsymbol{N}_{\mathrm{space}|l}$, and we arrive at $\boldsymbol{G}_{\mathrm{ZF}l} = \boldsymbol{H}_{\mathrm{ZF}l} \boldsymbol{H}_{\mathrm{ZF}l}^{\mathrm{H}}$, a scalar that defines the effective channel-gain for antenna l. For terminal k, we can compare the sum effective channel-gain from both of its antennas to γ from the BDZF case.

Furthermore, the eigenvalues of the measured channels' outer product can be used for dimensionality evaluations. Based on the channel matrix $\boldsymbol{H}$ ($\boldsymbol{H}_{\mathrm{ZF}l}$ in the CZF case), the outer product for a single antenna l, seeing the channel $\boldsymbol{h}_l$ is given by $\boldsymbol{O}_l = \boldsymbol{h}_l \boldsymbol{h}_l^{\mathrm{H}}$, an $M \times M$ matrix. The outer product for a single snapshot has a unit rank. A matrix with the size of the outer product can have a rank of at most M. By averaging the outer products over the C_s orientations and rotation angles for a measured condition, $\widetilde{\boldsymbol{O}}_l = \frac{1}{C} \sum_{c=1}^{C} \boldsymbol{h}_l(c) \boldsymbol{h}_l(c)^{\mathrm{H}}$, all available dimensions become included. The energy distribution of the eigenvalues of $\widetilde{\boldsymbol{O}}_l$ indicates how many dimensions are needed to represent all the channels included in C_s. The approach is similar to a sample covariance matrix. If we normalize the trace of $\widetilde{\boldsymbol{O}}_l$ to unity, $\widetilde{\boldsymbol{O}}_l' = \frac{1}{\mathrm{tr}(\widetilde{\boldsymbol{O}}_l)} \widetilde{\boldsymbol{O}}_l$, the magnitude of each eigenvalue will directly reflect the fraction of energy the said eigenmode carries.

The number of dimensions carrying the essential part of the energy relates to the number of clusters and indicates the richness of the environment. With $\widetilde{\boldsymbol{O}}_l'$ being Hermitian, an eigen-decomposition (ED) yields both the eigenvalues and the eigenvectors, $\mathrm{ED}(\widetilde{\boldsymbol{O}}_l') = \boldsymbol{U}_l \boldsymbol{\Lambda}_l \boldsymbol{U}_l^{\mathrm{H}}$, where $\boldsymbol{U}_l$ is a unitary matrix containing the eigenvectors and $\boldsymbol{\Lambda}_l$ is a diagonal matrix with the eigenvalues along the diagonal. The energy projected from the ith eigenvector of antenna l, (i.e., $\boldsymbol{U}_{l,\mathrm{col}:i}$) on the normalized matrix $\widetilde{\boldsymbol{O}}_j'$ of antenna j is

$$P_{l \to j,i} = \boldsymbol{U}_{l,\mathrm{col}:i}^{\mathrm{H}} \widetilde{\boldsymbol{O}}_j' \boldsymbol{U}_{l,\mathrm{col}:i}. \qquad (2)$$

We are aware that the estimation of dimensions from sampled measured data is a complex matter [14]. We assume that there is a direct relation between eigenmodes and clusters and that the SNRs are large enough to make relevant conclusions. The results are then used for relative comparisons rather than manifesting any absolute numbers.
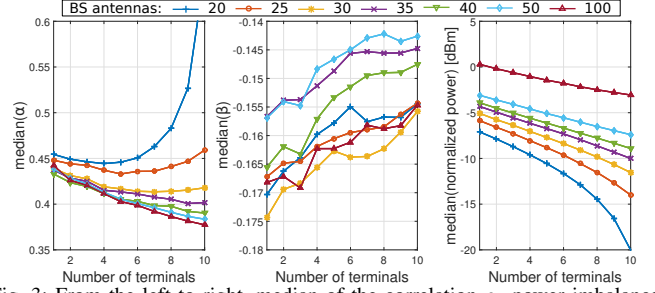

Fig. 3: From the left to right, median of the correlation α, power imbalance β and normalized channel-gain γ, as functions of the number of terminals (with BDZF) for a various number of BS antennas. The figures correspond to condition 2. The antenna selection is randomized from the array when $M < 100$.

III. EVALUATION RESULTS

A. The Influence of Multiple Users to the Channel

In Fig. 3, we show the medians of the terminal antenna correlation α, power imbalance β, and the normalized effective channel gain γ. The plots in Fig. 3 are functions of the total number of terminals, K, using BDZF for a various number of BS antennas, M. When the number of BS antennas is at least twice that of the streams present, a decrease in correlation as a function of the number of terminals can be observed. A lower number of antennas at the BS can not easily resolve the streams, and the correlation increases as more streams are introduced. For $M > 40$, the plots seem to converge to one curve, and therefore adding more antennas at the BS side will not significantly change the terminal antenna correlation α.

The power imbalance of the terminal antennas is not significantly influenced by the number of terminals or BS antennas. On the other hand, the gain drops as more terminals are introduced. Its dependence on the number of BS antennas for $M > 40$ relates to array gain and the more BS antennas the stronger the gain. It is also possible to determine when MaMi properties apply from the gain plots. When the curvature (2nd order derivative) increases so-called favorable propagation cannot be assumed, which also here suggests $M > 40$.

The results are consistent with our hypothesis, that the BDZF and plausibly also CZF allocate power to weaker clusters when the number of streams is increased, in a limited environment. For different terminal antenna designs or loading scenarios, however, the correlation may behave differently. From our results shown in Fig. 4, where each of the four conditions is used as reference terminal, the correlation is either unaffected by the number of terminals or drops, while the power imbalance only shows a minor dependency. It should be noted, that even if the decrease in correlation improves the capacity of the effective channel, the reduction in channel strength reduces it by a much larger extent and the net capacity typically decreases.

The channel strength for CZF without the BD is also interesting as it relaxes the processing burden on the terminal. The terminal will then receive an independent stream at each antenna. With BD, the UE needs to co-process the signals of its antennas. It can in such a case address the eigenmodes of the effective channel and reach the capacity of the effective channel with optimal power-allocation. The two plots to the
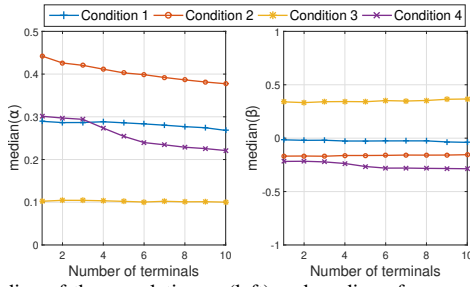
Fig. 4: Median of the correlation α (left) and median of power imbalance β (right), as functions of the number of terminals for 100 BS antennas, and the four alternative conditions. Note that the curves corresponding to condition 2 are the same as those in Fig. 3 for M=100.

Fig. 6: Number of eigenvectors from an antenna condition that are needed to represent the energy in other antennas (left). The energy becomes distributed among the eigenvectors as the number of terminals increases (right). CZF precoding has been used at the BS side in both cases.
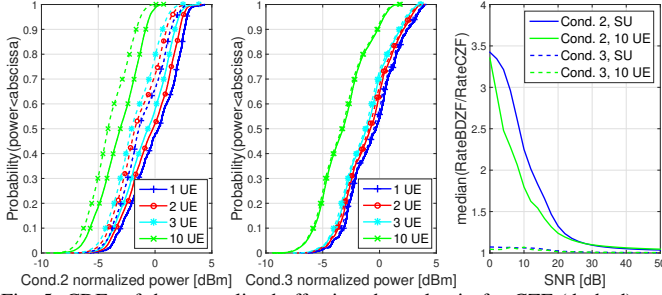

Fig. 5: CDFs of the normalized effective channel-gain for CZF (dashed) and BDZF (solid) case. To the left for condition 2, high correlation, and at the center condition 3, low correlation. To the right, the ratio of the median rates for the BDZF/CZF as a function of the SNR.

left in Fig. 5 show CDFs of the normalized effective channel-gain for both the CZF case (dashed lines) and the BDZF case (solid lines), for $K \in \{1, 2, 3, 10\}$ terminals. The left plot represents condition 2, for which the terminal antenna correlation is in the range 0.35 to 0.45. The center plot represents condition 3, for which the correlation is about 0.1.

As the correlation decreases from 0.45 to 0.35 in the left figure, corresponding to the SU case and the 10-terminal case, the difference in the effective channel-gain between the CZF and BDZF cases also decreases. The difference in the median is about 2 dB for the SU case, while, only about 1 dB for the 10 terminal case. The figures indicate that when the correlation is larger it is advantageous to address the eigenmodes rather than using CZF. Indeed, for terminal condition-2 the rate can be improved by more than a factor of three, depending on the signal-to-noise-ratio (SNR). This is shown in the right plot of Fig. 5, where the ratio between the median of the rates of the BDZF and CZF cases is plotted for condition-2 and condition-3, as a function of the SNR.

B. Common Clusters as a Function of Inter-Terminal Distance

The dimensionality of the signal subspace, in terms of the number of effective clusters or eigenvectors (assumed strongly related), is hard to estimate from inner product-based measures, since it influences the distributions of α, β, and γ through second-order phenomena, e.g. slope or curvature. Therefore, we look directly at the energy represented by the eigenvectors of the averaged outer products, based on (2). The plot to the left in Fig. 6 shows how many eigenvectors, ordered according to the strength of the eigenvalues computed from one of the terminal antennas, that are needed to represent
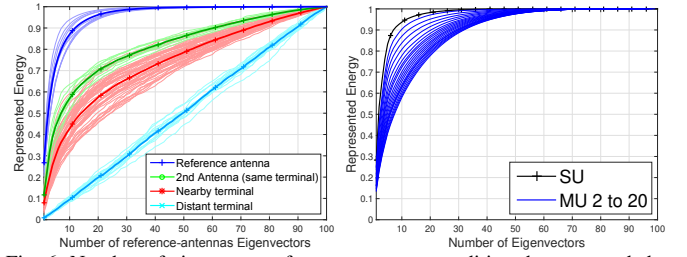
the energy seen by any other antenna. It can be noted that in this case there is no precoder involved and hence we are studying the physical channels. There are four populations of curves in the plot together with the average for the respective population. The first category, the blue curves, shows the accumulated energy for a selection of antennas as the ordered eigenvectors derived from their channels increases. The 10 strongest eigenvectors represent in average 87% of the energy. The small variation among the curves suggests that the number of dominating/effective clusters present is similar in all cases.

The green curves represent how well the ordered eigenvectors of one antenna can represent the energy of a second antenna, measured at the same time and located in the same terminal. In average 57% of the energy is represented by the 10 strongest eigenvectors. Also, in this case we see a small variation, suggesting that the number of dominant physical clusters seen by all antenna pairs is about the same.

The red curves represent how well the sorted eigenvectors of one antenna can represent the energy of a second antenna, which is located in a different terminal, measured at the same location (and therefore not measured simultaneously). In average 43% of the energy is represented by the 10 strongest eigenvectors. Again, the slope is steep at the beginning for all curves, suggesting that there are a few dominant common physical clusters. The facts that the antennas are not in the same terminal and that the measurements are not made simultaneously are likely contributions to the larger variation among the curves. In average, the correlation between the antennas of different users at the same location is also expected to be smaller than when in the same terminal, which, will lower the number of shared physical clusters. For both the green and red curves, the initial steep slope suggests that channels share the most dominant clusters.

The cyan curves represent how well the ordered eigenvectors of one antenna can represent the energy of a second antenna at a different location, measured in the same room about 5 meters apart. In this case, the curves become straight lines. This suggests that different clusters are dominant, or at least independent, in the different positions and no correlation between the channels can be observed. Thus, our results indicate that in a large auditorium, terminals spaced 5 meters apart may very well not share any clusters. There is a clear trend that co-located terminals seem to share more clusters.

The right plot in Fig 6 shows the accumulated energy for one of the antennas as the sorted eigenvectors derived

from the channel increases. The curves represent the different number of interfering streams, with CZF precoder at the BS. As, the number of streams increases, ranging from 1 to 20, more eigenvectors are needed to represent the same amount of energy. The figure is generated as an average, where the antennas are randomly selected from a set of measurements performed in a limited space. These results are in line with those based on the inner product and is consistent with our hypothesis that the energy becomes more evenly distributed among the effective eigenvectors as the number of streams increases also in the CZF case. Based on the relation between eigenvectors and clusters, this result suggests that the number of effective clusters increases with the number of simultaneous streams in a CZF precoded system.

IV. Conclusions

The results from the measurement-based analysis are consistent with the hypothesis: With a single terminal, the effective channel properties (i.e., correlation, power imbalance, and channel-gain) are consistent with the results from a cluster model when only a few dominant clusters are present. In multi-user situations, the results correspond to the case when also weaker clusters contribute to the effective channel.

The results explain the large discrepancy in the estimated number of clusters [13] between a precoded channel with a single terminal and that reported in [24] performed in the same environment. While the number of clusters in the physical channel may be large, precoded channels rely on a few strong clusters and the number of active clusters depends on the number of active streams. It is therefore important that realistic channel models for multiplexed operation include both dominant and weaker clusters in a given environment.

The results show that 40 BS antennas are sufficient in our environment with 20 streams/users and beyond that only the array-gain increases. We also showed that 20 streams can be resolved with only an array-gain penalty and no reduction in channel dimensionality. We found that block-diagonalized-zero-forcing can give a significant advantage compared to conventional zero-forcing even when the antennas within a terminal have a very low envelope correlation coefficient. Finally, a study of the outer products of the effective channel matrix supports that terminals close to each other share more clusters.

V. Acknowledgement

References

[1] T. L. Marzetta, "Noncooperative Cellular Wireless with Unlimited Numbers of Base Station Antennas OFDM," *IEEE Trans. Wireless Commun.*, vol. 9, no. 11, pp. 3590–3600, Nov. 2010, doi: http://dx.doi.org/10.1109/TWC.2010.092810.091092.

[2] *Study on New Radio (NR) Access Technology*, 14th ed., ETSI, 3GPP TR 38.912, 2017.

[3] E. G. Larsson, F. Tufvesson, O. Edfors, and T. L. Marzetta, "Massive MIMO for Next Generation Wireless Systems," *IEEE Communications Magazine*, vol. 52, no. 2, pp. 186–195, Feb. 2014, doi: http://dx.doi.org/10.1109/MCOM.2014.6736761.

[4] H. Q. Ngo, E. G. Larsson, and T. L. Marzetta, "Energy and Spectral Efficiency of Very Large Multiuser MIMO Systems," *IEEE Transactions on Communications*, vol. 61, no. 4, pp. 1436–1449, Apr. 2013, doi: http://dx.doi.org/10.1109/TCOMM.2013.020413.110848.

[5] F. Rusek, D. Persson, B. K. Lau, E. G. Larsson, T. L. Marzetta, O. Edfors, and F. Tufvesson, "Scaling Up MIMO: Opportunities and Challenges with Very Large Arrays," *IEEE Signal Processing Magazine*, vol. 30, no. 1, pp. 40–60, Dec. 2012, doi: http://dx.doi.org/10.1109/MSP.2011.2178495.

[6] E. Björnson, E. G. Larsson, and T. L. Marzetta, "Massive MIMO: 10 Myths and One Critical Question," *IEEE Communications Magazine*, pp. 114–123, Feb. 2016, doi: http://10.1109/MCOM.2016.7402270.

[7] E. G. Larsson, T. L. Marzetta, H. Yang, and H. Q. Ngo, *Fundamentals of Massive MIMO*, 1st ed. CAMBRIDGE UNIVERSITY PRESS, 2016.

[8] E. Björnson, J. Hoydis, and L. Sanguinetti, *Massive MIMO Networks: Spectral, Energy, and Hardware Efficiency*, 1st ed. now Publishers Inc., 2017.

[9] E. Björnson, J. Hoydis, M. Kountouris, and M. Debbah, "Massive MIMO Systems with Non-Ideal Hardware: Energy Efficiency, Estimation, and Capacity Limits," *IEEE Transactions on Information Theory*, vol. 60, no. 11, pp. 7112–7139, Nov. 2014, doi: http://dx.doi.org/10.1109/TIT.2014.2354403.

[10] E. L. Bengtsson, F. Tufvesson, and O. Edfors, "UE Antenna Properties and Their Influence on Massive MIMO Performance," in *Proceedings of the 9th European Conference on Antennas and Propagation, (EUCAP)*, Lisbon, Portugal, Apr. 2015, pp. 1–6.

[11] E. L. Bengtsson, P. C. Karlsson, F. Tufvesson, J. Vieira, S. Malkowsky, L. Liu, F. Rusek, and O. Edfors, "Transmission Schemes for Multiple Antenna Terminals in Real Massive MIMO System," in *Proceedings of GlobeCom 2016 Conference, IEEE Communications Society*, Washington DC, USA, Dec. 2016.

[12] À. O. Martínez, P. Popovski, J. Ø. Nielsen, and E. D. Carvalho, "Experimental Study of the Benefits of a Second Antenna at the User Side in a Massive MIMO System," *IEEE Access*, vol. PP, no. 99, pp. 1–1, 2017, doi: http://dx.doi.org/10.1109/ACCESS.2017.2785860.

[13] E. L. Bengtsson, F. Rusek, S. Malkowsky, F. Tufvesson, P. C. Karlsson, and O. Edfors, "A Simulation Framework for Multiple-Antenna Terminals in 5G Massive MIMO Systems," *IEEE Access*, vol. 5, pp. 26 819–26 831, 2017, doi: http://dx.doi.org/10.1109/ACCESS.2017.2775210.

[14] Q. H. Spencer, B. D. Jeffs, M. A. Jensen, and A. L. Swindlehurst, "Modeling the statistical time and angle of arrival characteristics of an indoor multipath channel," *IEEE Journal on Selected Areas in Communications*, vol. 18, no. 3, pp. 347–360, March 2000, doi: http://10.1109/49.840194.

[15] Y. Li, J. Zhang, and Z. Ma, "Clustering in Wireless Propagation Channel With a Statistics-Based Framework," in *2018 IEEE Wireless Communications and Networking Conference (WCNC)*, April 2018, pp. 1–6, doi: http://10.1109/WCNC.2018.8377218.

[16] K. Yu, Q. Li, D. Cheung, and C. Pretie, "On the Tap and Cluster Angular Spreads of Indoor WLAN Channels," *Proceedings IEEE Vehicular Technology Conference*, 2004.

[17] *Universal Mobile Telecommunications System UMTS Spatial channel model for Multiple Input Multiple Output MIMO simulations*, 12th ed., ETSI, 3GPP TR 25.996, 2014.

[18] J. Poutanen, J. Salmi, K. Haneda, V. Kolmonen, F. Tufvesson, and P. Vainikainen, "Propagation Characteristics of Dense Multipath Components," *IEEE Antennas and Wireless Propagation Letters*, vol. 9, pp. 791–794, 2010, doi: http://10.1109/LAWP.2010.2064751.

[19] A. F. Molisch, "A Generic Model for MIMO Wireless Propagation Channels in Macro- and Microcells," *IEEE Transactions on Signal Processing*, vol. 52, no. 1, pp. 61–71, Jan 2004, doi: http://dx.doi.org/10.1109/TSP.2003.820144.

[20] R. G. Vaughan and J. B. Andersen, "Antenna Diversity in Mobile Communications," *IEEE Transactions on Vehicular Technology*, vol. 36, no. 4, pp. 149–172, Nov. 1987, doi: http://dx.doi.org/10.1109/T-VT.1987.24115.

[21] Q. H. Spencer, A. L. Swindlehurst, and M. Haardt, "Zero-Forcing Methods for Downlink Spatial Multiplexing in Multiuser MIMO Channels," *IEEE Transactions on Signal Processing*, vol. 52, no. 2, pp. 461–471, Feb. 2004.

[22] J. Vieira, S. Malkowsky, K. Nieman, Z. Miers, N. Kundargi, L. Liu, I. Wong, V. Öwall, O. Edfors, and F. Tufvesson, "A Flexible 100-Antenna Testbed for Massive MIMO," in *Globecom Workshops (GC Wkshps)*, 2014, pp. 287–293.

[23] X. Gao, "Doctoral Thesis: Massive MIMO in Real Propagation Environments," *Series of Licentiate and Doctoral Theses*, 2016.

[24] A. Bordoux and et al., *D1.2 MaMi Channel Characteristics: Measurement Results*, final ed., FP7 EU project 619086, MAMMOET, Jun. 2015.